PAPER

Impact of GVD on the Performance of 2-D WH/TS OCDMA Systems Using Heterodyne Detection Receiver

Ngoc T. DANG[†a)], *Student Member*, Anh T. PHAM[†], *and* Zixue CHENG[†], *Members*

SUMMARY   In this paper, a novel model of Gaussian pulse propagation in optical fiber is proposed to comprehensively analyze the impact of Group Velocity Dispersion (GVD) on the performance of two-dimensional wavelength hopping/time spreading optical code division multiple access (2-D WH/TS OCDMA) systems. In addition, many noise and interferences, including multiple access interference (MAI), optical beating interference (OBI), and receiver's noise are included in the analysis. Besides, we propose to use the heterodyne detection receiver so that the receiver's sensitivity can be improved. Analytical results show that, under the impact of GVD, the number of supportable users is extremely decreased and the maximum transmission length (i.e. the length at which BER $\leq 10^{-9}$ can be maintained) is remarkably shortened in the case of normal single mode fiber (ITU-T G.652) is used. The main factor that limits the system performance is time skewing. In addition, we show how the impact of GVD is relieved by dispersion-shifted fiber (ITU-T G.653). For example, a system with 32×1 Gbit/s users can achieve a maximum transmission length of 111 km when transmitted optical power per bit is -5 dBm.
key words: *two-dimensional optical CDMA (2-D OCDMA), wavelength hopping/time spreading (WH/TS), heterodyne detection receiver, group velocity dispersion (GVD), fiber Bragg gratings (FBGs)*

1. Introduction

Optical code division multiple access (OCDMA) is a promising technique for next generation optical access networks [1]. Two-dimension wavelength hopping/time spreading (2-D WH/TS) OCDMA system is one kind of OCDMA systems that uses 2-D coding approach [2]. The 2-D codes are spread in both the time and frequency domains simultaneously, hence achieve better code performance in terms of both cardinality and correlation properties in comparison with that of the one-dimension (1-D) counterparts [3].

In 2-D WH/TS OCDMA system, the chip rate, though much lower compared with that in the 1-D systems, is still high. In addition, optical chip pulses are transmitted on different wavelengths. The system performance therefore will be affected by fiber dispersion caused by the difference of group velocities of different wavelengths, a phenomenon referred to as group velocity dispersion (GVD) [4]. The impact of GVD includes pulse broadening, peak power reduction, and time skewing, as illustrated in Fig. 1. Of these effects, the time skewing, the relative temporal shifting of optical pulses on difference wavelengths, is an exclusive phe-
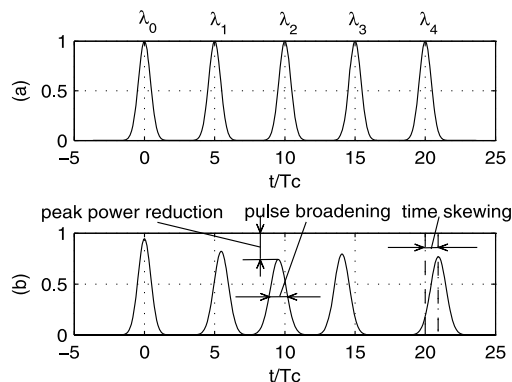
Fig. 1   Impact of GVD on multi-wavelength OCDMA signal: (a) the original signal and (b) the signal under the impact of GVD.

nomenon in OCDMA systems using multi-wavelength signal due to its decoding operation [5].

1.1 Related Works and Our Proposal

There has been a number of works studying the impact of fiber dispersion on the OCDMA systems, and the 2-D WH/TS OCDMA system in particular [5]–[9].

In the OCDMA systems using single wavelength, such as time spreading [6], [7] and spectral phase encoding systems [8], analysis of the impact of fiber dispersion focused on the traditional effects of pulse overlapping caused by pulse broadening and peak power reduction. However, in the OCDMA systems using multiple wavelengths, besides pulse broadening and peak power reduction, the impact of time skewing should be taken into consideration.

The first study on the impact of time skewing in the 2-D WH/TS OCDMA system was reported by Eddie K.H. Ng. et al. [5]. Based on coding theory the authors did an investigation the impact of temporal skewing on a code's auto- and cross-correlation properties. As well, they proposed methods for combating the deleterious effects of temporal skewing. In this work, however, the impact of pulse broadening and peak power reduction were not included. In addition, the analysis, which is purely based on coding theory without considering the impacts of any other noise and pulse propagation, is far from the real circumstances.

Later, the impact of pulse broadening and time skewing were investigated separately by simulation [9]. The simulation result shown that time skewing effect strongly degrades the performance of the 2-D WH/TS OCDMA system. For

3-wavelength and 7-chip-time optimized code, it was shown that a 10-Gchip/s system is limited to under 4 kilometers. As this is a simulation work, the condition is, to some extent, inflexible, for example only three simultaneous users was assumed, and preset optimized codes was used.

In this paper, we therefore propose to use a realistic model of pulse propagation in order to comprehensively analyze the impact of GVD on the performance of 2-D WH/TS OCDMA system. This model should be able to analyze all three effects of GVD, including pulse broadening, peak power reduction, and time skewing. Additionally, numerous noise and interferences, including multiple access interference (MAI), optical beating interference (OBI), and receiver's noise will be included in the analysis. Besides, we propose to use the heterodyne detection receiver so that the receiver's sensitivity can be improved and more users can be accommodated [10], [11]. As a matter of fact, under the impact of OBI, the 2-D WH/TS OCDMA systems using direct detection receiver is severely degraded and apparently unable to accommodate more than 10 users [12].

1.2 Main Contributions

A novel model of Gaussian pulse propagation in optical fiber is proposed. Based on this model, we comprehensively analyze the impact of all GVD effects on the performance of 2-D WH/TS OCDMA systems. Also, various parameters are investigated in the analysis, including maximum transmission length, number of supportable users, required optical power, and power penalty. In addition, we include both normal single-mode fiber (SMF) (ITU-T G.652 [21]) and dispersion-shifted fiber (DSF) (ITU-T G.653 [22]) in the analysis.

It is seen that under the impact of GVD, the number of supportable users is extremely decreased and the maximum transmission length is remarkably shortened in the case of normal SMF. We find that the main factor that limits the system performance is time skewing. We also discover that although the impact of pulse broadening and peak power reduction can be significantly relieved when DSF is used, the impact of time skewing is still relative strong. A power penalty of up to 6.4 dB is seen in the 2-D WH/TS OCDMA system with 32×1 Gbit/s users and the optical fiber length is 100 km.

The rest of the paper is organized as follows. Section 2 presents the descriptions of the 2-D WH/TS OCDMA system using heterodyne detection receiver. The performance analysis and numerical results are presented in Sects. 3 and 4, respectively. Finally, Sect. 5 concludes the paper.

2. System Descriptions

2.1 2-D WH/TS Code

The 2-D WH/TS code is characterized by a combination of time spreading and wavelength hopping patterns. This combination has several advantages: cross-correlation is reduced, the autocorrelation sidelobes are nonexistent and the cardinality of the code is greatly increased. There are several types of 2-D WH/TS code such as extended quadric congruence sequences [2], codes generated from "depth-first search algorithm" [13], pseudo-orthogonal matrix codes [14], and extended carrier hopping prime codes [15]. In this paper, we use prime code [16], which is the most popular and widely studied, for both time spreading and wavelength hopping.

For the time spreading patterns, each code is a sequence of p_s blocks and each block has exactly p_s chips (i.e. the sequence length is $N = p_s^2$), where p_s is a prime number. In each of these blocks, there exists only one chip pulse (i.e. the chip value is "1"). The positions of chip pulses in blocks of a code are determined by one of p_s spreading patterns, which are constructed of prime sequences corresponding to the prime number p_s.

A similar scheme is used for creating wavelength hopping patterns using a prime number p_h, which is also the number of available wavelengths. Each chip pulse is assigned to one of p_h wavelengths. We only consider the case of $p_s \leq p_h$. This mean that every wavelength appear in a code only one at the most. The selection of wavelengths for a code is determined by one of $p_h - 1$ hopping patterns because the hopping pattern that produces the same wavelength for all chip pulses is not used.

As a result, for a given set of prime numbers p_s, p_h, we can have a 2-D WH/TS code set whose cardinality of $p_s \times (p_h - 1)$, autocorrelation peak of p_s, and maximum cross-correlation of one [16].

An example of 2-D WH/TS codes when $p_s = 5$ and $p_h = 5$ is shown in Table 1. In this example, a single time spreading pattern (10000 01000 00100 00010 00001) is used for $p_h - 1$ wavelength hopping patterns.

2.2 2-D WH/TS OCDMA System

A schematic diagram of an 2-D WH/TS OCDMA system is shown in Fig. 2. There are K pairs of transmitter and receiver corresponding to K users in the system. A star optical coupler is used to distribute the optical signal from one transmitter to all receivers. When the optical signal propagates from the transmitter to the receiver, its power will be decreased because of the fiber attenuation and splitter losses. Let P_0, α, L be the transmitted power, the fiber attenuation coefficient, and the transmission length, respectively, the received power can be calculated as $P_s = [P_0 \exp(-\alpha L)]/K$.

A block diagram of a pair of transmitter and receiver in the 2-D WH/TS OCDMA system using heterodyne de-

Table 1 2-D WH/TS codes: $p_h - 1$ hopping patterns (HP) with one spreading pattern.

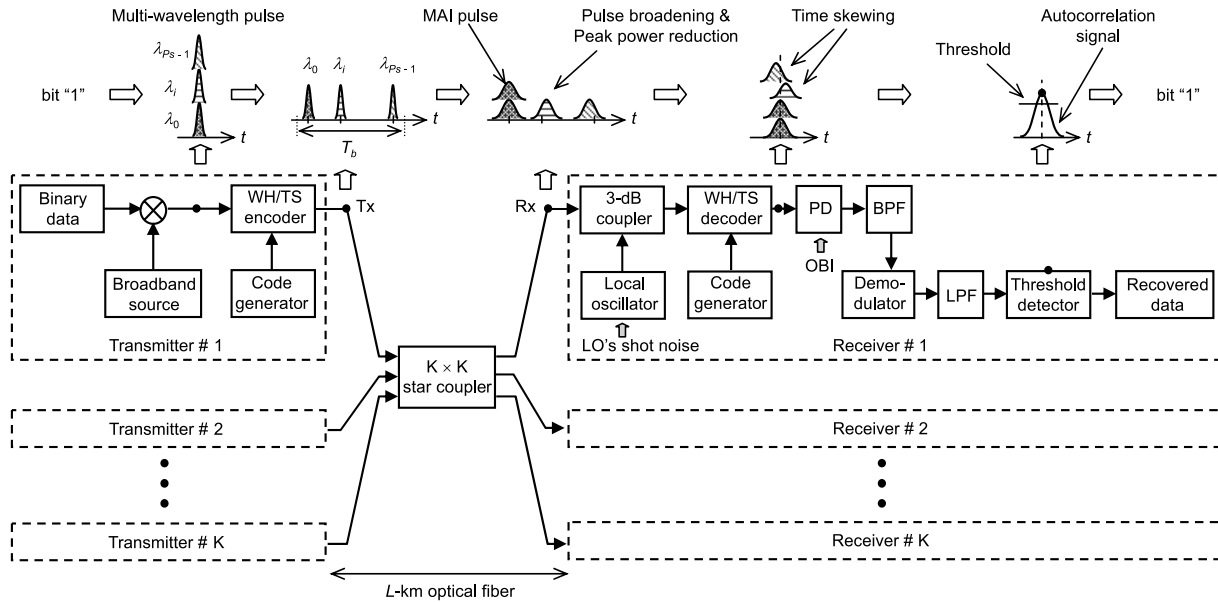|	block 0	block 1	block 2	block 3	block 4
HP 1	$\lambda_0 0000$	$0\lambda_1 000$	$00\lambda_2 00$	$000\lambda_3 0$	$0000\lambda_4$
HP 2	$\lambda_0 0000$	$0\lambda_2 000$	$00\lambda_4 00$	$000\lambda_1 0$	$0000\lambda_3$
HP 3	$\lambda_0 0000$	$0\lambda_3 000$	$00\lambda_1 00$	$000\lambda_4 0$	$0000\lambda_2$
HP 4	$\lambda_0 0000$	$0\lambda_4 000$	$00\lambda_3 00$	$000\lambda_2 0$	$0000\lambda_1$

Fig. 2 Schematic diagram of an 2-D WH/TS OCDMA system using heterodyne detection receiver.
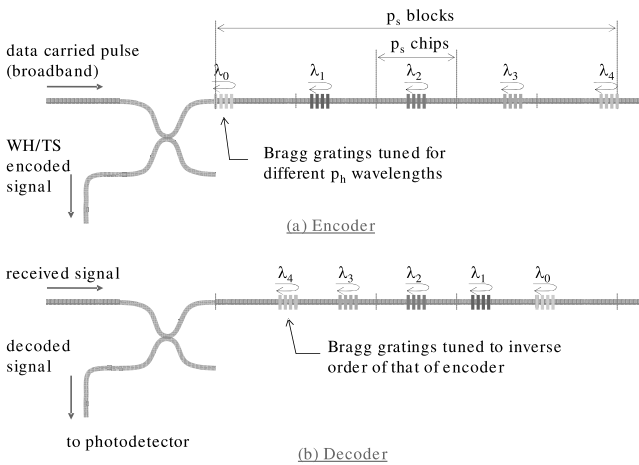

Fig. 3 FBG-based WH/TS encoder and decoder.

tection receiver is also illustrated in Fig. 2. At the transmitter, multi-wavelength signal from broadband source is modulated by binary data to generate on-off keying (OOK) signal. The broadband source used in this paper can be achieved with sinusoidal amplitude-phase hybrid modulation technique [17]. The OOK signal is then 2-D WH/TS encoded at a WH/TS encoder using a code generated by the code generator. The WH/TS encoder of the system are based on a linear array of fiber Bragg gratings (FBGs) and further detailed in Fig. 3(a). In the encoding operation, bit "0" is unchanged while wavelengths of bit "1" signal are time-delayed and tuned at different FBGs of the WH/TS encoder. The time-delays (i.e. the positions of the FBGs in the array) and the tuned wavelengths of FBGs are determined by the time spreading and hopping patterns of the code, respectively. Wavelengths are then combined and the encoded signal is transmitted into optical channel together with sig-

nals from other users.

At the receiver, the received signal (including MAI) is first mixed coherently with a local oscillator (LO). The LO is also a broadband source whose characteristics (spectra, wavelengths, and separation between them) are the same as the one at the transmitter. The mixed signal is then decoded at a WH/TS decoder (Fig. 3(b)), which also consists of the same array of FBGs, but these FBGs are positioned in an inverse order. When the received signal is passed through the WH/TS decoder, wavelengths from the desired user will be matched and the desired signal will be reconstructed by canceling the relative time delays among chip pulses. Wavelengths from interfering users that are either unmatched or differently delayed will be removed. On the other hand, those pulses whose wavelengths are matched and delays are coincided, will be collected and become MAI. The decoded signal, which consists of both desired and MAI pulses, is converted into an electrical signal by a photodetector (PD). It is at the PD, OBI will occur due to the beating between chip pulses with nearly the same wavelengths. The photocurrent is passed through a bandpass filter (BPF) to filter out crosstalks, converted to the baseband by demodulator, and then followed by a low-pass filter (LPF). Finally, the binary data is recovered by a threshold detector. The demodulation can be carried out either synchronously and asynchronously, however, for the simplicity of calculation, we will only consider the synchronous case in this paper.

It is necessary to note that when propagating along the optical fiber, optical chip pulses, both desired and MAI ones, are distorted by the impact of GVD. This distortion will consequently affect to the system performance hence should be considered for a comprehensive system performance analysis.

3. System Performance Analysis

In this section, we theoretically analyze the performance of the 2-D WH/TS OCDMA system using heterodyne detection receiver and derive its bit error rate (BER). As mentioned in the previous section, the impact of GVD will be taken into consideration along with other noise and interferences, including MAI, OBI, and receiver's noise.

It is necessary to note that our system is in the dispersion-dominant regime where the impact of nonlinear effects can be neglected. The reason is that the transmitted pulse power is relatively small (thanks to the use of heterodyne detection receiver) and the pulse width is not too short [19]. In fact, as the bit rate per user of 1 Gbit/s is used and the sequence length of 49 chips (i.e. $p_s = 7$) is chosen, the pulse width of 10 ps or higher can be set. Besides, for the sake of simplicity, we assume the polarization-matching case, the effect of polarization mode dispersion is thus also ignored. Also, we assume the chip synchronous case, i.e. the upper bound performance [3], for all users.

3.1 Pulse Propagation Model

An optical pulse can be approximated as Gaussian shape, and its propagation model in a dispersive medium can be expressed as [4]

$$s(t) = \sqrt{P_s} \frac{T_0}{(T_0^2 - j\beta_2 L)^{1/2}} \exp\left(-\frac{t^2}{2(T_0^2 - j\beta_2 L)}\right), \quad (1)$$

where P_s is received peak power and L is transmission length. T_0 is the half-width of pulse (at 1/e-intensity point) and β_2 is GVD parameter. From this equation we can see that, optical pulse remains its shape when propagating along optical fiber. Nevertheless, its width and peak power are moderated by the GVD parameter β_2.

This conventional model is good for analyzing pulse broadening and peak power reduction effects in single-wavelength or wavelength-independent systems (such as WDMA system). In 2-D WH/TS OCDMA system, however, besides these effects, it is also necessary to reflect the relative temporal shifting between two pulses (i.e. time skewing effect).

In order to describe time skewing effect, a new parameter reflecting the relative temporal shifting between two pulses needs to be calculated and added to the conventional model. We first select an arbitrary wavelength to be the reference one, e.g. λ_r. Without loss of generality, we assume the position of the reference wavelength in the time spreading sequence to be stationary during propagation. The relative temporal shifting between a wavelength λ_i and the reference one can be expressed as $(\beta_{1i} - \beta_{1r})L = \Delta\beta_{1i}L$, in which L is the transmission length, $\beta_{1r} = 1/v_{gr}$ and $\beta_{1i} = 1/v_{gi}$ with v_{gr} and v_{gi} are group velocities of the reference and i-th wavelength, respectively.

Our proposed modified model with the new parameter

for the optical pulse at wavelength λ_i ($0 \leq i \leq p_s - 1$), denoted as $s_i(t)$, then can be expressed as

$$s_i(t) = \sqrt{P_s} \frac{T_0}{(T_0^2 - j\beta_{2i}L)^{1/2}} \exp\left(-\frac{(t - \Delta\beta_{1i}L)^2}{2(T_0^2 - j\beta_{2i}L)}\right). \quad (2)$$

Another form of Eq. (2), which can be seen more clearly, is written as follows

$$s_i(t) = \sqrt{P_s}|A_i(t)| \exp(j\phi_{si}), \quad (3)$$

where $|A_i(t)|$ and ϕ_{si} are the normalized amplitude and phase of chip pulse at wavelength λ_i. $A_i(t)$ is expressed as

$$A_i(t) = \frac{T_0}{(T_0^2 - j\beta_{2i}L)^{1/2}} \exp\left(-\frac{(t - \Delta\beta_{1i}L)^2}{2(T_0^2 - j\beta_{2i}L)}\right). \quad (4)$$

It is worth noting that an optical pulse consists of two components: (1) a slowly varying amplitude, $s_i(t)$, of the pulse envelope (i.e. modulating signal) and (2) an optical carrier corresponding to the wavelength λ_i [19]. In our system, the spectral width of optical carriers depends on the reflection bandwidth of FBGs, which is as narrow as 0.1 nm (12.5 GHz) [18]. This spectral width is indeed much smaller than that of the modulating signal and its broadening effect hence is negligible [19]. Therefore, the optical carriers in the studied system can be assumed to be quasi-monochromatic (i.e. having single wavelength). The amplitude of optical pulse, whose wavelength is λ_i, is now fully expressed as

$$s_i(t) = \sqrt{P_s}|A_i(t)| \exp[j(\omega_i t + \phi_i)], \quad (5)$$

where ω_i is optical frequency of the optical carrier corresponding to the wavelength λ_i. The phase component ϕ_i includes phase of laser source and ϕ_{si} (in Eq. (3)).

3.2 Heterodyne Detection Receiver

As discussed in Sect. 2.2, the received optical signal is mixed coherently with a LO then passes through the WH/TS decoder before it falls on photodetector. In order to see how the mixing is carried out, we first consider the optical signals at the input of photodetector (Fig. 2).

At this point, after passing through the WH/TS decoder, optical pulses that contribute to autocorrelation peak consists of desired and MAI pulses. There are p_s desired pulses, one pulse appears at each wavelength, i.e. total p_s wavelength are visible. Again, without loss of generality, the desired user's wavelengths can be denoted from 0 to $p_s - 1$. Let k be the total number of MAI pulses at p_s wavelengths, where the number of MAI pulses at wavelength λ_i is denoted as k_i ($0 \leq i \leq p_s - 1$). k_i is the random variable ($0 \leq k_i \leq k$) and $k = \sum_{i=0}^{p_s-1} k_i$.

In order to express desired and MAI pulses, we used our proposed pulse propagation model (Eq. (5)). We denote ω_{di}, ϕ_{di} as optical frequency and phase of the optical carrier corresponding to the wavelength λ_i of the desired user; as well, denote ω_{cij}, ϕ_{cij} as optical frequency and phase of the

optical carrier corresponding to the wavelength λ_i of an interfering user j-th (out of k_i), respectively, where $j = (1, ..., k_i)$. The total decoded signal then can be expressed as

$$E_s(t) = \sum_{i=0}^{p_s-1} \sqrt{P_s} |A_i(t)| \exp[j(\omega_{di}t + \phi_{di})]$$
$$+ \sum_{i=0}^{p_s-1} \sum_{j=1}^{k_i} \sqrt{P_s} |A_i(t)| \exp[j(\omega_{cij}t + \phi_{cij})]. \quad (6)$$

The first part of Eq. (6) is the desired signal whereas the second one presents MAI. Here, to simplify the calculation, we assume that transmitted power levels of any wavelengths are the same for all users. Also, the distance from all transmitters to the receiver is the same (L km). The received peak power and the normalized amplitude of optical pulse at wavelength λ_i are the same for every user.

The LO at a specific receiver has p_s wavelengths corresponding to p_s wavelengths of its desired user's. We denote frequencies and phases of wavelengths of the LO as ω_{LOi}, ϕ_{LOi} with $i = (0, 1, ..., p_s - 1)$. For the sake of simplicity, we assume the powers are the same level at all wavelengths of the LO. The photocurrent at the output of the photodetector after removing constant direct-current (DC) component and cross talk can be expressed as

$$i = 2\mathfrak{R} \sum_{i=0}^{p_s-1} \sqrt{P_{LO}P_s} |A_i(t)| \cos(\omega_{IFd}t + \Delta\phi_{IFdi})$$
$$+ 2\mathfrak{R} \sum_{i=0}^{p_s-1} \sum_{j=1}^{k_i} \sqrt{P_{LO}P_s} |A_i(t)| \cos(\omega_{IFc}t + \Delta\phi_{IFcij})$$
$$+ 2\mathfrak{R} \sum_{i=0}^{p_s-1} \sum_{j=1}^{k_i} \sqrt{P_s P_s} |A_i(t)|^2 \cos(\Delta\omega_{dij}t + \Delta\phi_{dij})$$
$$+ 2\mathfrak{R} \sum_{i=0}^{p_s-1} \sum_{j=1}^{k_i} \sum_{m=j+1}^{k_i} \sqrt{P_s P_s} |A_i(t)|^2 \cos(\Delta\omega_{cijm}t + \Delta\phi_{cijm})$$
$$+ i_{rx}, \quad (7)$$

where $\mathfrak{R}$ denotes the photodiode responsivity; the intermediate frequencies and phases of data and j-th interfering user are $\omega_{IFd} = \omega_{di} - \omega_{LOi}$ and $\omega_{IFc} = \omega_{cij} - \omega_{LOi}$ as well as $\Delta\phi_{IFdi} = \phi_{di} - \phi_{LOi}$ and $\Delta\phi_{IFcij} = \phi_{cij} - \phi_{LOi}$ for $i = (0, 1, ..., p_s - 1)$; and the frequencies and phases of primary and secondary beating components are expressed as $\Delta\omega_{dij} = \omega_{cij} - \omega_{di}$, $\Delta\omega_{cijm} = \omega_{cij} - \omega_{cim}$ and $\Delta\phi_{dij} = \phi_{cij} - \phi_{di}$ and $\Delta\phi_{cijm} = \phi_{cij} - \phi_{cim}$ for any $m \neq j$ and $m, j \in (0, 1, ..., p_s - 1)$.

The first term in the Eq. (7) represents desired photocurrent and the second one represents the photocurrent caused by MAI. The third term is primary OBI representing the beating between desired pulses and MAI pulses. Each pulse at wavelength λ_i from the desired signal will beat with the k_i pulses from interfering signal. The fourth term is secondary OBI representing the beating among the MAI pulses. At particular wavelength λ_i there are k_i pulses beating again each other. Finally, the last term i_{rx} represents receiver's
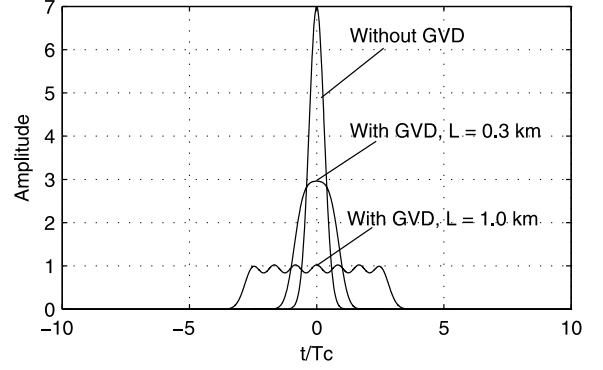

Fig. 4 Autocorrelation signal, $A_d(t)$, for the case using SMF. The prime sequence has $p_s = 7$.

noise which includes shot noise and thermal noise.

The photocurrent generated at the photodetector is passed through a BPF centered at the intermediate frequency (ω_{IF}). For synchronous demodulation, the photodetector is multiplied with $\cos(\omega_{IF}t)$ and filtered by a LPF to reject the components oscillating at $2\omega_{IF}$. The phase differences $\Delta\phi_{IFdi}$ and $\Delta\phi_{IFcij}$ generally varies randomly because of phase fluctuations associated with the signal phase and the LO phase. This fluctuations, called phase noise, will affect the performance of the system. The phase noise problem can be efficiently solved by using special receivers known as phase-diversity receivers [20]. Such receivers use two or more photodetectors whose outputs are combined to produce a signal that is independent of the phase difference. Therefore, in our analysis, in order to simplify the calculation, $\Delta\phi_{IFdi}$ and $\Delta\phi_{IFcij}$ are assumed to be zero and the effect of phase noise is neglected.

3.3 Signal to Noise Ratio

Firstly, we consider the desired current. Based on above assumption, the phase difference $\Delta\phi_{IFdi} = 0$, the desired current is hence given by

$$i_d(t) = 2\mathfrak{R} \sum_{i=0}^{p_s-1} \sqrt{P_{LO}P_s} |A_i(t)| = 2\mathfrak{R} \sqrt{P_{LO}P_s} A_d(t), \quad (8)$$

where $A_d(t) = \sum_{i=0}^{p_s-1} |A_i(t)|$ is autocorrelation signal.

In order to describe the impact of GVD on autocorrelation signal, an example is shown in Fig. 4, where autocorrelation signal is investigated for the case of $p_s = 7$. The autocorrelation peak is corresponding to $t = 0$ which is also the time of thresholding. Without the impact of GVD, the autocorrelation peak (without MAI) equals to the code weight, p_s. Under the impact of GVD, time skewing and peak power reduction will make the autocorrelation peak decrease. Especially, the impact of time skewing can be seen clearly in Fig. 4 for the case of $L = 1$ km. At the thresholding time, the value of desired current will be $I_d = 2\mathfrak{R} \sqrt{P_{LO}P_s} A_d$, where $A_d = A_d(0)$ is the peak of autocorrelation.

Besides desired current, MAI current also contributes

to autocorrelation peak. As $\Delta\phi_{IFcij}$ is assumed to be zero, MAI current hence can be calculated as

$$i_{MAI}(t) = 2\Re \sqrt{P_{LO}P_s} \sum_{i=0}^{p_s-1} k_i |A_i(t)|. \tag{9}$$

The MAI current at thresholding time is written by

$$I_{MAI} = 2\Re \sqrt{P_{LO}P_s} \sum_{i=0}^{p_s-1} k_i |A_i(0)|. \tag{10}$$

The value of $|A_i(0)|$ depends on MAI pulse's wavelength as shown in Eq. (4). Because the difference among β_{2i} is small, $|A_i(0)|$ has maximum value when $\Delta\beta_{1i} = 0$, which means that MAI pulse has the same wavelength with reference one. In this analysis, we will consider the worst case, all k MAI pulses are assumed to drop into reference wavelength. The value of $|A_i(0)|$ is now replaced by A_c, where A_c is received from Eq. (4) with $\Delta\beta_{1i} = 0$, $t = 0$, and β_{2i} equals to β_{2r} of reference wavelength. The MAI current is now expressed as

$$I_{MAI} = 2\Re \sqrt{P_{LO}P_s} k A_c. \tag{11}$$

When desired user transmits bit "1," the MAI is constructive. When the desired user's bit is "0," the MAI can lead to errors. The total of desired and MAI currents $I_b (b \in (0, 1))$ can be expressed as

$$I_b = bI_d + I_{MAI}. \tag{12}$$

Next, to calculate OBI power, distribution of k interfering pulses over p_s wavelengths should be considered. Denote $\kappa = (k_0, k_1, ..., k_{p_s-1})$ as the p_s dimensional vector that represents the distribution of k interfering pulses over p_s wavelengths. It is seen that κ is a random variable that can be modeled as a multinominal distribution with an equal probability $P_i = 1/p_s$ [12]. By averaging the secondary OBI component, the OBI power for two cases $b = 0$ and $b = 1$, which includes primary and secondary OBI, can be derived from [10] as

$$i_{OBIb}^2 = 2B_e\tau_c\Re^2 P_s^2 A_c^4 \left(bk + \frac{1}{p_s}\binom{k}{2}\right), \tag{13}$$

where B_e is photodetector electrical bandwidth and τ_c is coherent time of the broadband source which can be approximated as $\tau_c = 1/B_0$ where B_0 is the optical bandwidth.

Finally, we calculate the receiver noise power, which includes the contribution from both shot noise $i_s^2 \approx 2p_s eB_e\Re P_{LO}$ (note that the shot noise from the p_s LOs is dominant as $P_{LO} \gg P_s$) and thermal noise $i_{th}^2 = 8\pi k_B T_n B_e^2 C$ [11]. Where e is the electron charge, k_B is Boltzman's constant, T_n is the receiver noise temperature, and C is the receiver capacitor.

Total noise variance, i_{nb}^2 ($b \in (0, 1)$), is expressed as follows

$$i_{nb}^2 = i_{OBIb}^2 + i_s^2 + i_{th}^2. \tag{14}$$

Each bit is detected by comparing the autocorrelation peak with a threshold current I_D. The signal to noise ratio (SNR_b) for two cases ($b = 0$ and $b = 1$) at the thresholding time is calculated as

$$SNR_b = \frac{(I_b - I_D)^2}{i_{nb}^2}. \tag{15}$$

3.4 Bit Error Rate (BER)

We assume that there are $K - 1$ interfering users, i.e. the number of simultaneous users is K, in which i users (out of the possible $K-1$ interfering users) are sending "1." For any user, the probability of transmitting "0" or "1" is assumed to be equally likely. Therefore, i can be modeled as binominal variable with probability $1/2$. Among i interfering users sending bit "1," we assume that there are k pulses matched with desired user's code. Denote $\langle\mu_\lambda\rangle$ as the average number of wavelengths common to a pair of two codes, the probability that one pulse is matched with desired user's code is $\langle\mu_\lambda\rangle/p_s^2$. k thus can be also modeled as binominal variable with probability $\langle\mu_\lambda\rangle/p_s^2$.

In order to minimize the BER, we consider the case that I_D is optimum [19]. Moreover, the demodulated photocurrent as well as noises can be modeled as Gaussian random variables, the total probability of error hence can be calculated as [10]

$$P_e = \sum_{i=1}^{K-1} \binom{K-1}{i} 2^{-(K-1)} \sum_{k=1}^{i} \binom{i}{k}\left(\frac{\mu_\lambda}{p_s^2}\right)^k \left(1 - \frac{\mu_\lambda}{p_s^2}\right)^{i-k}$$
$$\times Q\left(\frac{I_1 - I_0}{i_{n1} + i_{n0}}\right), \tag{16}$$

where

$$Q(x) = \frac{1}{2\pi} \int_x^\infty \exp(-y^2/2)dy. \tag{17}$$

Here, I_1 and I_0 are I_b, the total of data and MAI currents derived from Eq. (12), corresponding to $b = 1$ and $b = 0$. The average number of wavelengths common to a pair of two codes μ_λ, in case of prime sequence with $p_s < p_h$, can be estimated as [2]

$$\mu_\lambda = \frac{1}{\binom{p_h}{p_s}}\left\{\binom{p_h-1}{p_s-1}\frac{(p_s-1)(p_s-2)+(p_h-2)}{p_h-2}\right.$$
$$\left. + \binom{p_h-1}{p_s}\frac{p_s(p_s-1)}{p_h-2}\right\}. \tag{18}$$

Note that in the case of $p_s = p_h$, the average number of wavelengths common to a pair of two codes, μ_λ, equals to p_s.

4. Numerical Results

For the numerical result, we use WH/TS sequences that have $p_s = 7$ and $p_h = 11$, i.e. the maximum number of users is 70. With the user bit rate is 1 Gbit/s and the sequence
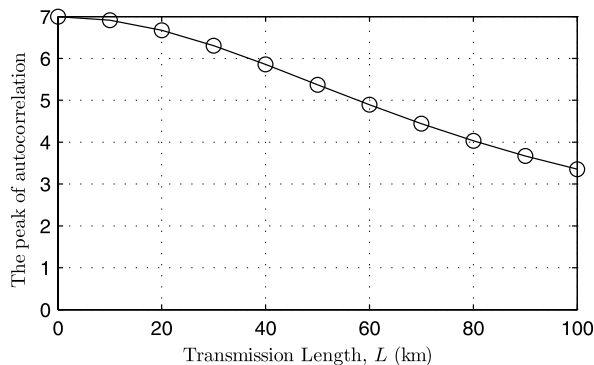
Fig. 5 The peak of autocorrelation, A_d, for the case of using DSF. The prime sequence has $p_s = 7$ and $p_h = 11$.

Table 2 System parameters and constants.

Name	Symbol	Value
Boltzmann's constant	k_B	1.38×10^{-23} W/K/Hz
Electron charge	e	1.6×10^{-19} C
Light velocity	c	3×10^8 m/s
Receiver capacitor	C	0.02×10^{-12} F
Noise temperature	T_n	300 K
PD responsivity	$\Re$	1 A/W
Bit rate per user	B_e	1 Gbit/s
Prime number for TS	p_s	7
Prime number for WH	p_h	11
LO optical power	P_{LO}	0 dBm

Fig. 6 BER versus transmission length (L) when $K = 32 \times 1$ Gbit/s users and $P_b = -5$ dBm. Transmission medium is SMF.

length equals to 49 (i.e. p_s^2), the chip duration is approximately 20 ps. Therefore, the full-width at half maximum of the chip pulse [4] can be chosen as 10 ps. The 11 wavelengths are at the window 1550 nm and range from 1445 nm to 1555 nm (i.e. the wavelength interval is 1 nm). In following analysis, considered user uses 7 wavelengths from 1447 nm to 1553 nm.

The transmission mediums used in the analysis are the standard ITU-T normal SMF (G.652) and DSF (G.653) with the attenuation is approximately 0.2 dB/km. The dispersion parameters are also based on ITU-T Recommendations. SMF has dispersion coefficient $D_{1550} = 17$ ps/nm × km and dispersion slope coefficient $S_{1550} = 0.056$ ps/nm^2 × km. DSF has zero dispersion at wavelength 1550 nm and dispersion slope coefficient $S_{1550} = 0.047$ ps/nm^2 × km.

Before analyzing the system performance, it is necessary to see how GVD affects on the autocorrelation signal. Figure 4 shows the normalized amplitude of autocorrelation signal for the case of SMF. The peak of autocorrelation signal strongly decreases when the transmission length (L) increases. When the transmission length is 300 m, the peak of autocorrelation drops to 3. For $L = 1$ km, the autocorrelation signal is composed of seven peaks instead of single sharp one. This is because each chip pulse travels at different group velocity.
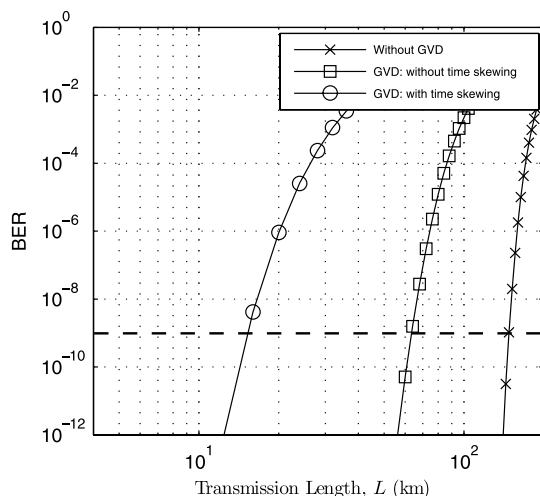
In order to reduce the impact of GVD, DSF with small dispersion coefficient is recommended. Figure 5 illustrates how DSF relieves the impact of GVD. The reduction of autocorrelation peak is not as much as that of SMF. At 100-km DSF, the autocorrelation peak is still larger than that of 300-m SMF.

Investigating the impact of GVD on autocorrelation signal is necessary but not enough. When an optical access system is designed, important parameters that need to be determined are maximum transmission length (i.e. the length at which BER $\leq 10^{-9}$ can be maintained), the number of supportable users, and required optical power (or power penalty). To make our analysis more comprehensive, we will investigate system's BER versus these parameters for two cases: using SMF and DSF.

The system parameters and constants used in following

analysis are shown in Table 2. In order to have fair comparison with other systems, the numerical results are considered under a constraint on power per information bit. Under this constraint, the transmitted power per chip P_0 can be derived from transmitted power per bit P_b as $P_0 = P_b/p_s$.

4.1 Analytical Results for the Case of SMF

We first investigate the maximum transmission length when the system is affected by GVD and the SMF is used. Figure 6 shows the system's BER vs. the transmission length when the transmitted power per bit $P_b = -5$ dBm and the number of users $K = 32 \times 1$ Gbit/s users. In order to analyze different GVD effects on the system performance, three cases of BER: without GVD, with pulse broadening and peak power reduction effects (these two effects occur concurrently), and with full impact of GVD (including time skewing), are shown.

It is seen that when only pulse broadening and peak power reduction effects are considered, the maximum transmission length of the analyzed system is reduced from 147 to 63 km, which is still considered good enough for systems like access networks. However, when time skewing effect is included, it is extremely shortened to 15.5 km. This reveals that the time skewing is dominant effect in the 2-D WH/TS
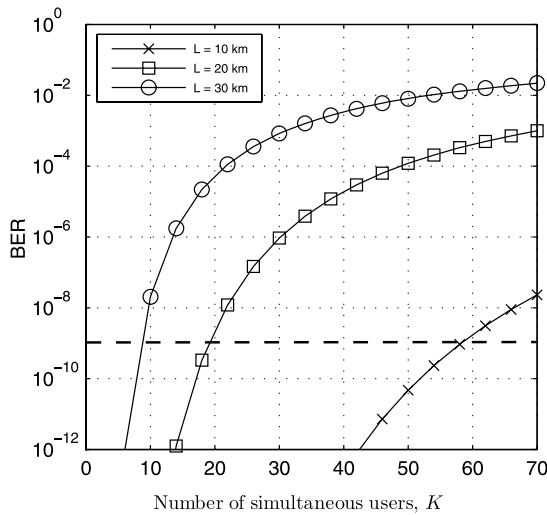
Fig. 7 BER versus number of simultaneous users (K) when $P_b =$ -5 dBm. The user bit rate is 1 Gbit/s and transmission medium is SMF.
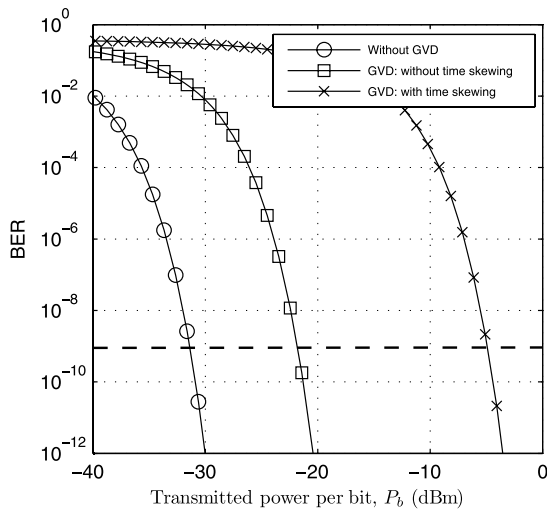

Fig. 8 BER versus number transmitted power per bit (P_b) when $K =$ 32 users and $L = 15.5$ km. The user bit rate is 1 Gbit/s and transmission medium is SMF.

OCDMA systems. Additionally, if no dispersion compensation method is used, the 2-D WH/TS OCDMA systems cannot be implemented on the current optical networks, which are mainly based on SMF.

Next, we show the reduction of the number of supportable users when the transmission length increases in Fig. 7. We keep the transmitted power per bit $P_b = -5$ dBm and increase L from 10 to 20 and 30 km. The number of supportable users will decrease from 58 to 19 and 9 users respectively. With this tendency, the system can supports only a few users when $L = 40$ km.

Figure 8 shows the system's BER versus transmitted power per bit when $K = 32 \times 1$ Gbit/s users and $L = 15.5$ km. Although the impact of pulse broadening and peak power reduction are not as much as that of time skewing, its power penalty is considerable, i.e. 11 dB in the total of 27 dB is
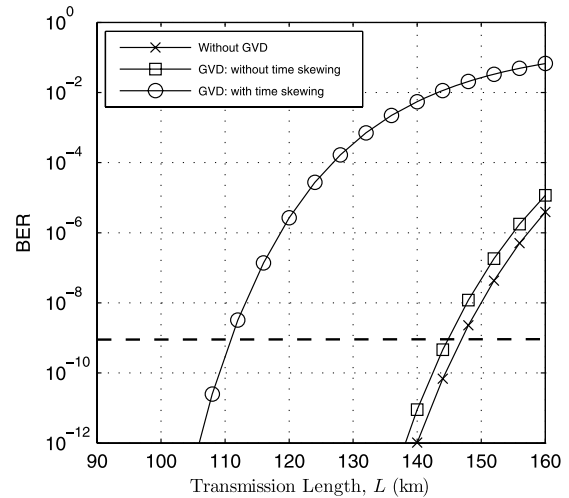
Fig. 9 BER versus transmission length (L) when $P_b = -5$ dBm and $K =$ 32×1 Gbit/s users. Transmission medium is DSF.

shown. This is due to high dispersion coefficient of SMF and relative small pulse width (i.e. 10 ps).

4.2 Analytical Results for the Case of DSF

In the previous section, we showed that the transmission length and number of users are very limited when SMF is used. We will now investigate BER of the system using DSF and compare with the case of SMF to find how the impact of GVD is relieved.

As depicted in Fig. 9, the impact of pulse broadening and peak power reduction is significantly relieved when DSF is used. In comparison with the case of without GVD, the transmission length is only 2 kilometers shorter (i.e. 145 km compared with 147 km). In addition, the impact of time skewing is also reduced, which make the total impact of all GVD effects remarkably decrease. With the same transmitted power per bit ($P_b = -5$ dBm), the system using DSF can support 32 users with the maximum transmission length of 111 km. It is 7 times greater than that of using SMF.

Figure 10 illustrates the system's BER against the number of simultaneous users when $P_b = -5$ dBm and the user bit rate is 1 Gbit/s. In comparison with Fig. 7, the system using DSF can support more number of users as well longer transmission length compared with the system using SMF. For example, the system using DSF can support 32 users at $L = 111$ km compared with 19 users at $L = 20$ km of the system using SMF.

Finally, we investigate system's BER against transmitted power per bit when $L = 111$ km and $K = 32$ users. In order to keep BER $\leq 10^{-9}$ it is required to increase transmitted power to compensate power reduction because of GVD effects. As shown in Fig. 11 the power penalty of pulse broadening and peak power reduction is negligible. However, the impact of time skewing is still relatively strong. A power penalty of up to 7 dB is seen in the 2-D WH/TS OCDMA system with 111-km optical fiber length. More detail about
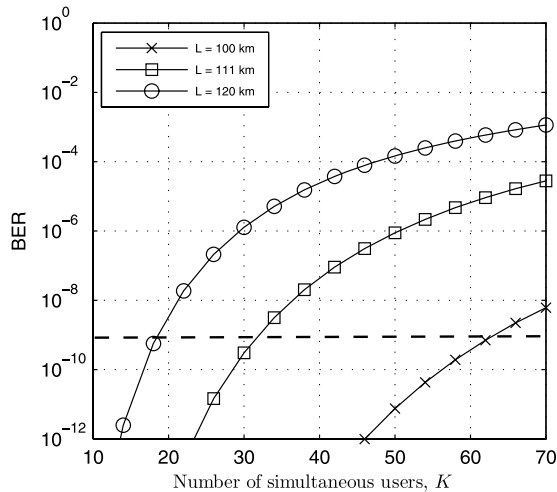
Fig. 10 BER versus number of simultaneous users (K) when $P_b = -5$ dBm. The user bit rate is 1 Gbit/s and transmission medium is DSF.
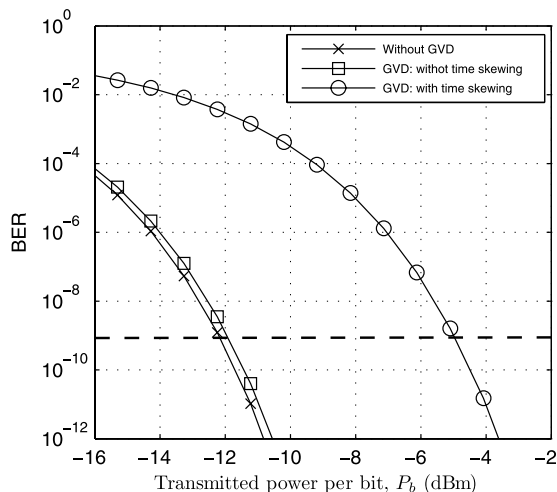
Fig. 11 BER versus number transmitted power per bit (P_b) when $K = 32$ users and $L = 111$ km. The user bit rate is 1 Gbit/s and transmission medium is DSF.
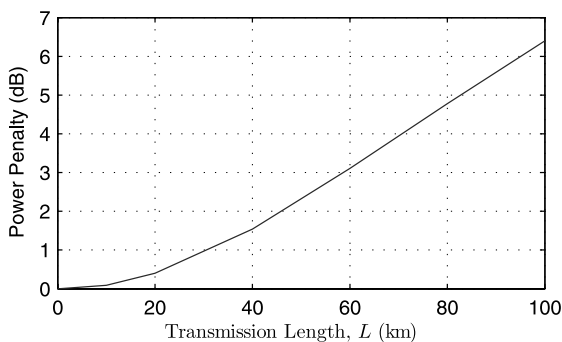
Fig. 12 Power penalty versus transmission length (L) when $K = 32 \times 1$ Gbit/s users. Transmission medium is DSF.

the power penalty versus transmission length under the impact of GVD for the case of DSF is illustrated in Fig. 12.

5. Conclusions

We have presented a comprehensive study of the impact of GVD on the performance of the 2-D WH/TS OCDMA system. A realistic model of Gaussian pulse propagation is proposed and heterodyne detection receiver is used so that the receiver's sensitivity can be improved. First, the impact of GVD on optical pulse propagating in optical fiber was analyzed. Then the system performance was investigated taking into account various kinds of noise and interferences, including MAI, OBI, and receiver's noise. The results show that, under the impact of GVD, the number of supportable users is extremely decreased and the maximum transmission length is remarkably shortened in the case of normal single mode fiber is used. The main factor that limits the system performance is time skewing.

Although the impact of pulse broadening and peak power reduction is almost compensated by dispersion-shifted fiber, the impact of time skewing is relatively strong. Moreover, the cost of using DSF may be ineffective. Therefore, alternate techniques, such as pre-skewing at encoder and post-skewing at decoder, are desired so that the systems can use low-cost SMF. Dispersion compensating techniques are also required to work with reconfigurable devices. In our future research, we plan to study how to solve this issue.

Acknowledgments

References

[1] A. Stok and E.H. Sargent, "The role of optical CDMA in access networks," IEEE Commun. Mag., vol.40, no.9, pp.83–87, Sept. 2002.

[2] L. Tancevski and I. Andonovic, "Hybrid wavelength hopping/time spreading schemes for use in massive optical networks with increased security," IEEE J. Lightwave Technol., vol.14, no.12, pp.2636–2647, Dec. 1996.

[3] J.A. Salehi, "Code division multiple-access techniques in optical fiber networks. Part II. Systems performance analysis," IEEE Trans. Commun., vol.37, no.8, pp.834–842, Aug. 1989.

[4] G.P. Agrawal, Nonlinear Fiber Optics, Academic, San Diego, CA, 2001.

[5] E.K.H. Ng, G.E. Weichenberg, and E.H. Sargent, "Dispersion in multiwavelength optical code division multiple-access systems: Impact and Remedies," IEEE Trans. Commun., vol.50, no.11, pp.1811–1816, Nov. 2002.

[6] F.B. Mezger and M.B. Pearce, "Dispersion limited fiber-optic CDMA systems with overlapped signature sequences," Proc. IEEE LEOS 9th Annu. Meeting, pp.408–409, 1996.

[7] S.P. Majumder, A. Azhari, and E.H. Hossam, "The impact of fiber chromatic dispersion on the BER performance of an optical CDMA IM/DD transmission system," IEEE Photonics Technol. Lett., vol.17, no.6, pp.1340–1342, June 2005.

[8] Y. Igarashi and H. Yashima, "Dispersion compensation for ultrashort

light pulse CDMA communication systems," IEICE Trans. Commun., vol.E85-B, no.12, pp.2776–2784, Dec. 2002.

[9] A. Sahin and A.E. Willner, "System limitations due to chromatic dispersion and receiver bandwidth for 2-D time-wavelength OCDMA systems," Proc. IEEE LEOS 16th Annu. Meeting, vol.2, pp.551–552, Oct. 2003.

[10] A.T. Pham and H. Yashima, "Performance analysis of 2-D WH/TS OCDM systems using prime sequences and a heterodyne detection receiver," Proc. IEEE 49th Annu. Global Telecomm. Conf., pp.1–6, 2006.

[11] A.T. Pham and H. Yashima, "Performance anhancement of the 2-D WH/TS synchronous OCDM system using a heterodyne detection receiver and PPM signaling," OSA J. Optical Networking, vol.6, no.6, pp.789–800, June 2007.

[12] L. Tancevski and L.A. Rusch, "Impact of the beat noise on the performance of 2-D optical CDMA systems," IEEE Commun. Lett., vol.4, no.8, pp.264–266, Aug. 2000.

[13] R.M.H. Yim, L.R. Chen, and J. Bajcsy, "Design and performance of 2-D codes for wavelength-time optical CDMA," IEEE Photonics Technol. Lett., vol.14, no.5, pp.714–716, May 2002.

[14] A.J. Mendez, R.M. Gagliardi, V.J. Hernandez, C.V. Bennett, and W.J. Lennon, "Design and performance analysis of wavelength-time (W/T) matrix codes for optical CDMA," IEEE J. Lightwave Technol., vol.21, no.11, pp.2524–2533, Nov. 2003.

[15] W.C. Kwong and G.C. Yang, "Extended carrier-hopping prime codes for wavelength-time optical code-division multiple access," IEICE Trans. Commun., vol.52, no.7, pp.1084–1091, July 2004.

[16] G.C. Yang and W.C. Kwong, Prime Code With Application to CDMA Optical and Wireless Networks, Artech House, 2002.

[17] M. Fujiwara, J. Kani, H. Suzuki, K. Araya, and M. Teshima, "Flattened optical multicarrier generation of 12.5 GHz spaced 256 chanel based on sinusoidal amplitude and phase hybrid modulation," IEEE Electron. Lett., vol.37, no.15, pp.967–968, June 2001.

[18] J. Magné, D.P. Wei, S. Ayotte, L.A. Rusch, and S. LaRochelle, "Experimental demonstration of frequency-encoded optical CDMA using superimposed fiber bragg gratings," Proc. OSA Topical Meeting on Bragg Gratings, Photosesivity, and Poling, pp.1–3, 2003.

[19] G.P. Agrawal, Fiber-Optic Communication Systems, Third ed., John Wiley & Sons, 2002.

[20] L. Kazovsky, "Phase- and polarization-diversity coherent optical techniques," IEEE J. Lightwave Technol., vol.7, no.2, pp.279–292, Feb. 1989.

[21] ITU-T Recommendation G.652, Characteristics of a single-mode optical fibre and cable, June 2005.

[22] ITU-T Recommendation G.653, Characteristics of a dispersion-shifted single-mode optical fibre and cable, Dec. 2006.

Ngoc T. Dang was born in Nam Dinh, Vietnam, in 1976. He received the B.E. degree from Hanoi University of Technology in 1999 and the M.E. degree from Posts and Telecommunications Institute of Technology (PTIT) in 2005, both in Electronics Engineering. He is currently working towards a Ph.D. degree in Computer Network Systems at the University of Aizu, Japan. From 1999 to 2007, he worked as a lecturer at PTIT. His present research interests are in the area of spread spectrum technique and optical communications. Dang receives Japanese government scholarship (MonbuKagaku-sho) for his Ph.D. study. He also received scholarship from Vietnamese government and Vietnam Posts and Telecommunications Corp. for undergraduate study.

Anh T. Pham was born in Thanh Hoa, Vietnam, in 1975. He received the B.E. and M.E. degrees, both in Electronics Engineering from the Hanoi University of Technology, Vietnam in 1997 and 2000, respectively, and the Ph.D. degree in Information and Mathematical Sciences from Saitama University, Japan in 2005. From 1998 to 2002, he worked as a Telecommunication Network Engineer for NTT Vietnam Corp. Since April 2005, he has been an Assistant Professor at the School of Computer Science and Engineering, The University of Aizu. His present research interests are in the area of spread spectrum technique and optical communications. Dr. Pham received Japanese government scholarship (MonbuKagaku-sho) for Ph.D. study. He also received Vietnamese government scholarship for undergraduate study.

Zixue Cheng (Shigaku Tei) received the M.E. and Ph.D. degrees from Tohoku university in 1990 and 1993, respectively. He was an assistant professor from 1993 to 1999, an associate professor from 1999 to 2002, and has been a professor, since Feb. 2002, at the School of Computer Science and Engineering, University of Aizu. Currently he is interested in distributed algorithms, distance education, ubiquitous computing, and functional safety. Dr. Cheng is a member of IEEE, ACM, and IPSJ.